6198 J. Med. Chem. 2010, 53, 6198–6209
DOI: 10.1021/jm100601q

Journal of Medicinal Chemistry Article

"Clicked" Bivalent Ligands Containing Curcumin and Cholesterol As Multifunctional Aβ Oligomerization Inhibitors: Design, Synthesis, and Biological Characterization

James A. Lenhart,[†] Xiao Ling,[†] Ronak Gandhi,[†] Tai L. Guo,[‡] Phillip M. Gerk,[§] Darlene H. Brunzell,[‡] and Shijun Zhang*,[†]

[†]*Department of Medicinal Chemistry,* [‡]*Department of Pharmacology and Toxicology, and* [§]*Department of Pharmaceutics, Virginia Commonwealth University, Richmond, Virginia 23298*

Received May 17, 2010

In our effort to develop multifunctional compounds that cotarget beta-amyloid oligomers (AβOs), cell membrane/lipid rafts (CM/LR), and oxidative stress, a series of bivalent multifunctional Aβ oligomerization inhibitors (BMAOIs) containing cholesterol and curcumin were designed, synthesized, and biologically characterized as potential treatments for Alzheimer's disease (AD). The in vitro assay results established that the length of spacer that links cholesterol and curcumin and the attaching position of the spacer on curcumin are important structural determinants for their biological activities. Among the BMAOIs tested, **14** with a 21-atom-spacer was identified to localize to the CM/LR of human neuroblastoma MC65 cells, to inhibit the formation of AβOs in MC65 cells, to protect cells from AβOs-induced cytotoxicity, and to retain antioxidant properties of curcumin. Furthermore, **14** was confirmed to have the potential to cross the blood−brain barrier (BBB) as demonstrated in a Caco-2 cell model. Collectively, these results strongly encourage further optimization of **14** as a new hit to develop more potent BMAOIs.

Introduction

Alzheimer's disease (AD[a]) is a devastating neurodegenerative disease and is the most common cause of dementia. The etiology of AD still remains elusive, and multiple factors have been suggested to contribute to the development of AD, among which amyloid-β (Aβ) and oxidative stress have been well documented.[1,2] Recently emerging evidence indicates that small Aβ oligomers (AβOs), rather than insoluble Aβ fibrils, are responsible for disruption of neuronal synaptic plasticity and the resulting early cognitive impairment associated with AD.[3] Studies of brain samples from AD patients also confirmed the correlation of AβOs with the severity of dementia.[4,5] Despite the fact that multiple assemblies of AβOs and a variety of underlying mechanisms have been suggested in the literature,[6−11] one point of consensus remains clear: the requirement of AβOs. Collectively, these findings provide compelling support for developing Aβ oligomerization inhibitors as novel therapeutic agents for the treatment of AD. Increased oxidative damage by reactive oxygen species (ROS) and reactive nitrogen species is another feature consistently found in the brains of AD patients.[2,12] Many factors have been demonstrated to cooperatively contribute to the production of ROS in the AD brain such as biometals, mitochondria dysfunction, and Aβ.[13] Transgenic mouse studies have also shown a correlation of increased oxidative stress and Aβ accumulation.[14]

Recently, a wealth of data has implicated the roles of neuronal cell membrane/lipid rafts (CM/LR) in the oligomerization and toxicity of Aβ.[15,16] Once associated with the membranes, Aβ exhibits an enhanced rate of aggregation that is dependent on pH, metal ion, and ganglioside interactions.[17−19] Recently, evidence has also indicated that lipid rafts, a cell membrane microdomain enriched in cholesterol and sphingolipids, can accelerate the cell membrane binding of Aβ and AβOs formation.[15,16] On the other hand, destruction of lipid rafts affects Aβ membrane binding and protects cells from Aβ toxicity.[20] Furthermore, Aβ precursor protein (APP), APP cleavage enzymes (β- and γ-secretases), Aβ and AβOs have all been identified in lipid rafts, suggesting that lipid rafts may be a critical platform for Aβ production and oligomerization.[21] In addition, oxidative stress has been shown to upregulate presenilin-1, the critical component of γ-secretase, in lipid rafts of neuronal cells to promote Aβ production.[22] Altogether, it is apparent that CM/LR are important regulators in

*Correspondence address: Shijun Zhang, Ph.D., Department of Medicinal Chemistry, School of Pharmacy, Virginia Commonwealth University, Richmond, Virginia 23298-0540. Tel: 804-6288266. Fax: 804-8287625. E-mail: szhang2@vcu.edu.

[a] Abbreviations: Aβ, amyloid-β; AβOs, amyloid-β oligomers; AD, Alzheimer's disease; APP, Aβ precursor protein; ATCC, American Type Culture Collection; BBB, blood−brain barrier; BMAOIs, bivalent multifunctional Aβ oligomerization inhibitors; CHO, Chinese hamster ovary; CM/LR, cell membrane/lipid rafts; CTX-B, cholera toxin subunit B; DAPI, 4′,6-diamino-2-phenylindole; DBU, 1,8-diazabicycloundec-7-ene; DCFH-DA, dichlorofluorescein diacetate; DIC, differential interference contrast; DMF, dimethylformamide; DMEM, Dulbecco's modified eagle's medium; DMSO, dimethyl sulfoxide; EDC, 1-ethyl-3-(3-dimethylaminopropyl)-carbodiimide; ELISA, sandwich enzyme-linked immunoassays; FBS, fetal bovine serum; HBSS, Hank's balanced salt solution; HOBt, hydroxybenzotriazole; HPLC, high performance liquid chromatography; NAC, N-acetylcysteine; NK, natural killer; PBS, phosphate buffered saline; PMA, phosphomolybdic acid; PVDF, polyvinylidene fluoride; ROS, reactive oxygen species; SDS−PAGE, sodium dodecyl sulfate−polyacrylamide gel electrophoresis; SEM, standard error of mean; TBS, Tris buffered saline; TC, tetracycline; TEM, transmission electron microscope; TFA, trifluoroacetic acid; THF, tetrahydrofuran; TLC, thin-layer chromatography; TMS, tetramethylsilane.

 Published on Web 07/28/2010

AD development and this relationship can be exploited to design and develop novel AD therapies.

Numerous chemical ligands have been developed as potential AD treatments by targeting Aβ and oxidative stress.[23,24] However, very few of them moved to clinical trials and none of them has been approved by FDA, which suggests that targeting a single risk factor is not an ideal strategy for developing treatments for this multifaceted disease. In contrast, new approaches that cotarget multiple risk factors involved in AD are emerging as promising strategies for developing effective treatment agents for AD.[25−27] Herein, we hypothesized that a bivalent multifunctional Aβ oligomerization inhibitors (BMAOIs) strategy that targets AβOs, oxidative stress, and CM/LR would be a novel approach to design strategically distinct ligands with the potential to overcome the limits posted by the traditional single-factor based approach. Conceptually, these BMAOIs contain a multifunctional AβO-inhibitor pharmacophore that accommodates additional antioxidant properties as well as a CM/LR anchor pharmacophore linked by a spacer (Figure 1). The use of bivalent strategies to explore protein−protein interactions has been particularly successful in opioid receptor research field.[28] Recently, this concept has been extended to neurodegenerative diseases in developing acetylcholinesterase inhibitors and metal chelators.[25] We envisaged that such BMAOIs would chaperone the multifunctional AβO-inhibitor moiety in close proximity to CM/LR in which AβOs and oxidative stress are produced to increase its accessibility to interfere with these multiple processes, thus improving its clinical efficacy (Figure 1). In this report, we rationally designed, synthesized, and biologically characterized a series of BMAOIs, and one compound was identified as a new hit for further investigation.

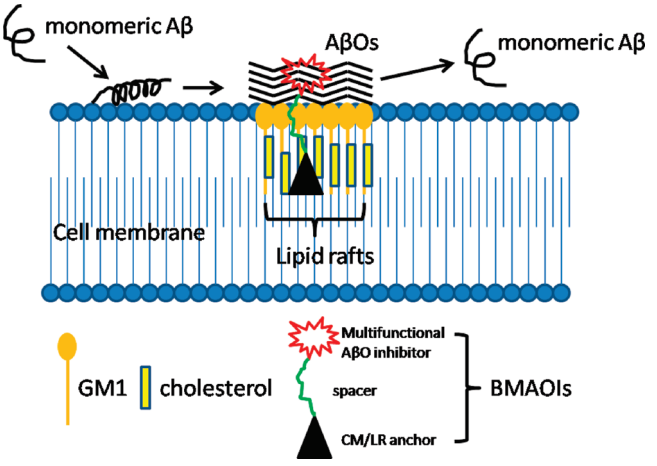

Figure 1. BMAOIs strategy and design.

Design and Chemistry

The desired BMAOIs must contain an AβO-inhibitor moiety with intrinsic antioxidant effects, as well as incorporate a residue able to efficiently interact with CM/LR, spanned by a stable linkage. Thus, in our designed BMAOIs, curcumin (**1**) was selected as the multifunctional AβO-inhibitor pharmacophore, and on the other end, connected by a spacer, cholesterol (**2**) was selected as the anchor pharmacophore to the CM/LR (Figure 2). The selections of **1** and **2** were based on the following reasons: (1) **1** is an important phytochemical that has long been known for its antioxidant, anti-inflammatory properties as well as recently discovered anti-Aβ properties;[29−32] (2) it has been demonstrated that **2** and

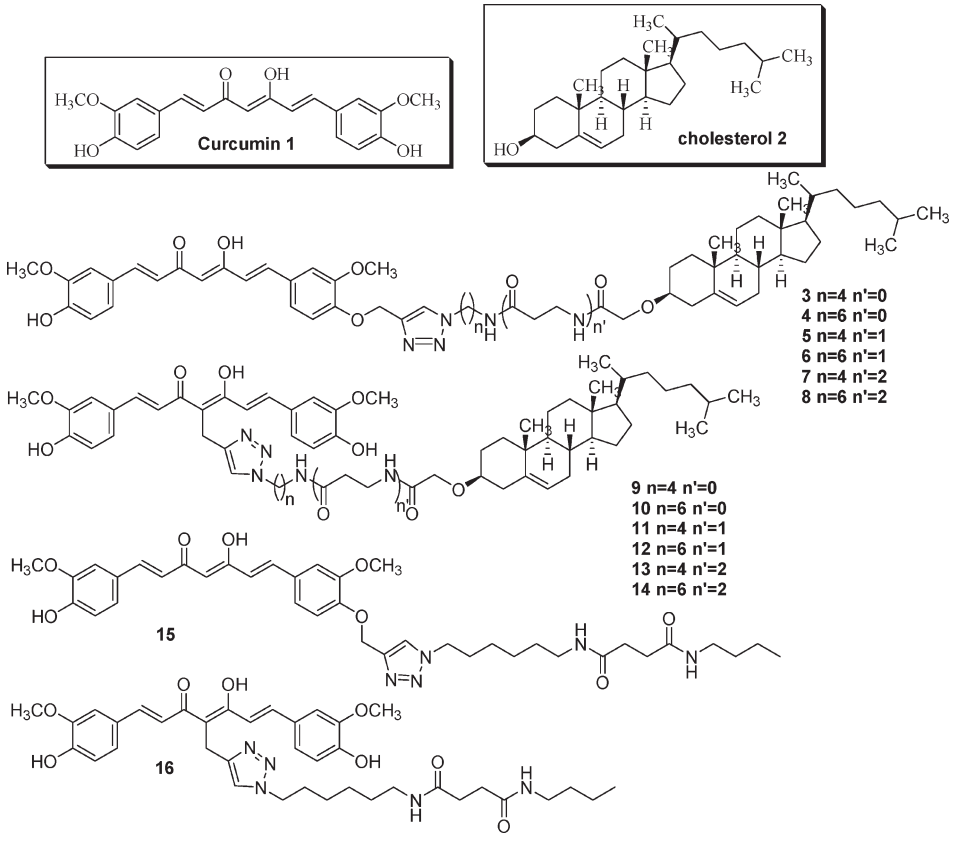

Figure 2. Chemical structures of **1**, **2**, designed BMAOIs and monovalent ligands.

Scheme 1. Synthesis of intermediates **20** and **23**[a]

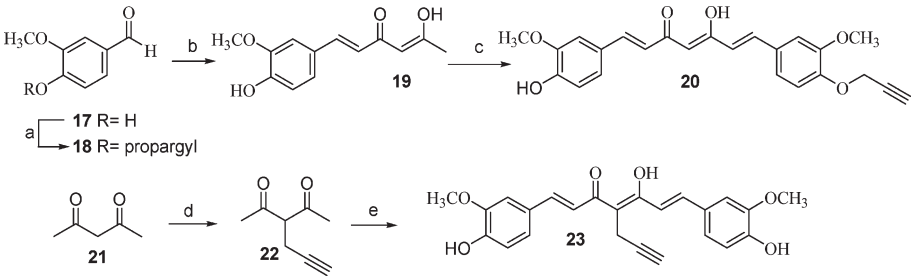

[a] Reagents and conditions: (a) propargyl bromide, K_2CO_3, DMF; (b) i. B_2O_3, acetylacetone; ii. $(BuO)_3B$, piperidine; iii. 1 N HCl; (c) i. B_2O_3, ii. 16, $(BuO)_3B$, piperdine; iii. 1 N HCl; (d) propargyl bromide, DBU, benzene; (e) i. B_2O_3, 17, $(BuO)_3B$, *n*-$BuNH_2$; ii. 1 N HCl.

other sterols linked with another moiety can anchor CM/LR in mammalian cells and function as a carrier to induce internalization via endocytosis.[33,34] The crucial consideration in designing BMAOIs is to determine the loci on the two pharmacophores for attaching the spacer and the nature and length of the spacer. Given the fact that alkylation of the 3-OH of **2**/sterol does not affect their binding affinities to CM/LR,[33,34] we selected this position as the spacer attachment position. On the other end, one of the phenolic oxygens and the C-4 position (methylene carbon between the two carbonyl groups) of **1** were selected to design two series of BMAOIs to investigate the optimal attachment. Since it is not clear whether Aβ oligomerization occurs on the surface or inside of CM/LR and optimal spacer length range cannot be predicted from the existing literature, we varied the spacer length as a key parameter for investigation. Since the cell membrane thickness is frequently cited as 3 nm (although ranging from 2.5 to 10 nm), we have decided to initially vary the spacer length from 11−21 atoms (Figure 2). Two monovalent ligands (**1** attached to spacer but not cholesterol) (**15** and **16**) were also designed to evaluate the influence of spacer attachment on **1**'s activity. Recently "click chemistry"[35] methodology has been successfully applied to connect **1** to peptides by Ouberai et al.[36] Therefore, to efficiently assemble the two pharmacophores together, we adopted this "click chemistry" methodology to include a 1,4-disubstituted triazole ring in the spacer.

The synthesis began with the preparation of alkyne intermediates **20** and **23** through a well established Pabon reaction (Scheme 1).[37] Briefly, alkylation of vanillin **17** with propargyl bromide provided **18**. Aldol reaction of **17** with 2,4-pentanedione followed by another Aldol reaction with **18** afforded intermediate **20**. Alkylation of 2,4-pentane-dione with propargyl bromide in the presence of 1,8-diazabicycloundec-7-ene (DBU) in benzene yielded **22** which on Aldol reaction with **17** afforded intermediate **23**.

As shown in Scheme 2, carboxylic acid **25** was synthesized following the reported procedure.[34] Then, coupling reactions of **25** with various azidoamines **26**−**31** which were synthesized through coupling reactions of azidoalkylamines **26** and **27** with Boc protected β-alanine followed by Boc deprotection afforded azido intermediates **32**−**37**.

Once all the required intermediates were available, the click reactions of the alkynes **20** or **23** with **32**−**37** were applied under sodium ascorbate and $CuSO_4$ in THF/H_2O conditions to obtain the designed BMAOIs **3**−**8** or **9**−**14**, respectively (Scheme 3). All the designed BMAOIs are in keto−enol forms in chloroform judged by ^{1}HNMR and ^{13}CNMR. The synthesis of the monovalent compounds **15** or **16** is similar to the synthesis of BMAOIs. Click reactions of **20** or **23** with azido intermediate **38** which was synthesized from the reaction of

Scheme 2. Synthesis of Intermediates **32**−**37**[a]

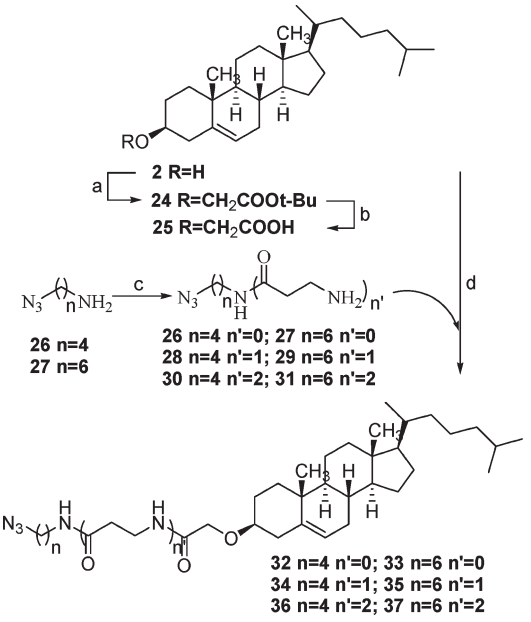

[a] Reagents and conditions: (a) *tert*-butyl-2-bromoacetate, NaH, THF; (b) formic acid/Et_2O; (c) i. Boc protected beta-alanine or Boc protected beta-alanylalanine, EDC, HOBt, CH_2Cl_2; ii. TFA/CH_2Cl_2; (d) EDC, HOBt, CH_2Cl_2.

butylamine with succinic anhydride followed by amide coupling with 6-azidohexylamine achieved the synthesis of **15** or **16**, respectively.

Results and Discussion

Inhibition of AβOs Production by Designed BMAOIs. The rational design of BMAOIs targeting CM/LR and AβOs as well as oxidative stress will require demonstration of anticipated effects in a biologically relevant system. The whole cell assay is a composite of not only Aβ oligomerization inhibition, but also permeability, stability, and other factors will validate the accessibility and function of our BMAOIs. MC65 is a human neuroblastoma cell line that conditionally expresses C99, the C-terminus fragment of APP using tetracycline (TC) as transgene suppressor.[38] Upon removal of TC, these cells can produce intracellular Aβ aggregates including small AβOs. Most importantly, the induced cytotoxicity in these cells by TC removal has been associated with the accumulation of AβOs.[39] Furthermore, oxidative stress has been indicated as one potential effector to impart neurotoxicity upon the accumulation of intracellular AβOs in these cells.[40] Therefore, MC65 cells were initially employed

Scheme 3. Synthesis of Designed BMAOIs and Monovalent Ligands[a]

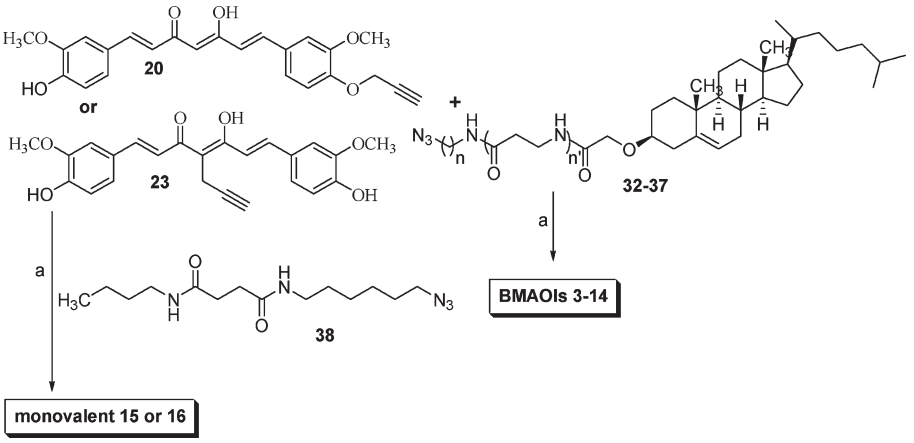

[a] Reagents and conditions: (a) $CuSo_4$, sodium ascorbate, THF/H_2O (1:1).

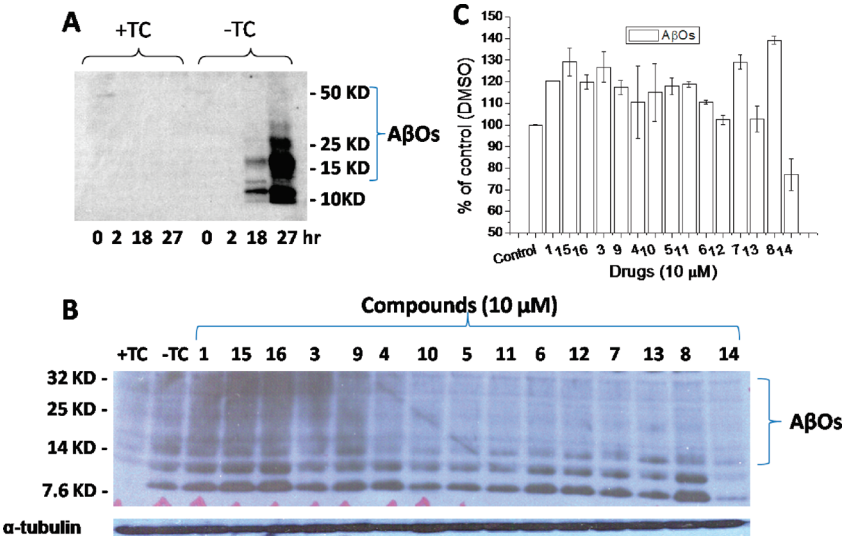

Figure 3. Inhibition of AβOs formation by **14** in MC65 cells and ML60 cells. (A) MC65 cells were cultured under +TC or −TC conditions for varying intervals (0, 2, 18, 27 h), and then cell lysates were analyzed by Western blot using 6E10 antibody. (B) MC65 cells were treated with indicated compounds (10 μM) for 24 h immediately after the removal of TC. Lysates from cultures were analyzed by Western blotting using 6E10 antibody. The image represents the results from one of three independent experiments. (C) ML60 cells were treated with test compounds (10 μM) for 24 h and extracellular AβOs in conditioned medium were analyzed by ELISA. Data were expressed as mean percentage of AβOs (n = 4) with parallel DMSO cultures set at 100%. Error bars represent standard error of mean (SEM).

to validate and test our BMAOIs using Western blot analysis. All BMAOIs were first evaluated at a single concentration of 10 μM. Candidate compounds with inhibitory activities at this concentration were further evaluated in a dose-dependent manner in the following assays. As shown in Figure 3A, withdrawal of TC induced the production of AβOs consistent with reported results.[39] **1** did not exhibit inhibition on the formation of AβOs (Figure 3B). Spacer attachment at both positions (**15** and **16**) did not change the activity of **1**. BMAOIs **3**, **4** and **9**, **10** (spacer length ranging from 11 to 13 atoms) showed no inhibition on the formation of small AβOs. BMAOIs **5**−**7** and **11**−**13** (spacer length ranging from 15 to 19 atoms) slightly inhibited the formation of AβOs with specific suppression of the 24-kDa bands. Notably, among the BMAOIs tested, **14** (with 21 atoms in the spacer) significantly inhibited AβOs production. This may indicate that spacer length is an important structural determinant for their inhibition on AβOs formation in MC65 cells with a 21-atom-spacer best supporting the design of BMAOIs tested here. Most importantly, it is notable that **8**, with the same spacer length (21 atoms) as **14** but different spacer attaching position on **1**, did not show inhibitory effects on AβOs formation, which suggests the importance of attachment position on **1** as well. Next, another cell line, ML60, was employed to evaluate the inhibition of AβOs production. ML60 cell line is a line of Chinese hamster ovary (CHO) cells stably expressing wild type APP and mutant presenilin 1 (M146L missense mutation) and can specifically produce high levels of extracellular AβOs.[41] As shown in Figure 3C, only **14** inhibited the production of extracellular AβOs in ML60 cells, and surprisingly all the other compounds increased the production of AβOs at a tested concentration (10 μM). It has been demonstrated that AβOs are formed intracellularly and then excreted outside the cells.[42] The results from ML60 cells may further reflect **14**'s ability to reduce intracellular AβOs, which is consistent with the results from MC65 cells. Altogether, these results suggest that spacer length and attachment position on **1** are important

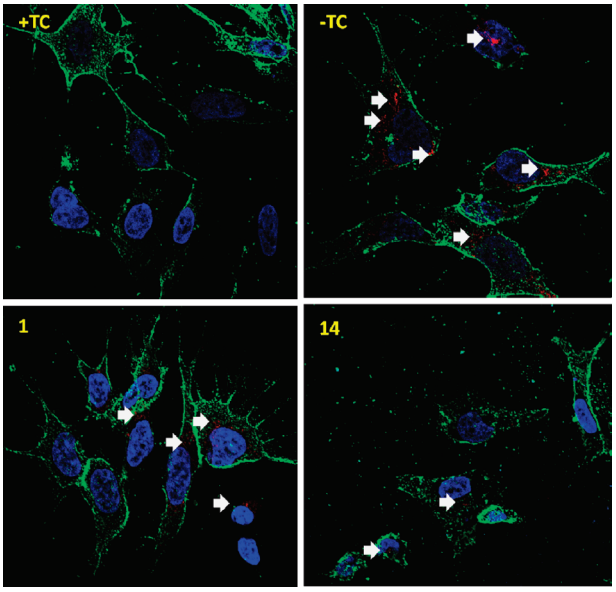

Figure 4. Immunocytochemistry of **1** and **14** in MC65 cells. MC65 cells were treated with the indicated compounds (10 μM) immediately after the removal of TC. After 24 h, the cells were fixed and immunofluorescently stained for AβOs (red), CM/LR (green), and nucleus (blue) and imaged with Leica TCS-SP2 AOBS confocal laser scanning microscope. White arrows indicate the red puncta of AβOs. The image represents one of five areas examined.

structural determinants for inhibitory activities on the formation of AβOs and BMAOIs with optimal spacer length can improve their potencies.

In order to further confirm the inhibition of small AβOs by **14** in MC65 cells, an AβO-specific antibody A11[43] combined with Alexa Fluor 568 conjugated secondary antibodies was employed to detect the expression of AβOs in MC65 cells using immunocytochemistry techniques. As shown in Figure 4, removal of TC induced rapid intracellular accumulation of AβOs (red fluorescence puncta). Consistent with Western blot results, **14** significantly inhibited the formation of AβOs in MC65 cells upon the removal of TC. Surprisingly, **1** slightly suppressed the formation of AβOs in this assay while it exhibited no inhibitory effects on the formation of AβOs in Western blot analysis. This might be due to the different antibodies used for detection in these two assays with A11 antibody more specific to AβOs. In addition to confirming Western blot data, these results also indicate that both **14** and **1** can cross the cell membrane of MC65 cells.

Interactions of 14 with AβOs and Cell Membrane of MC65 Cells. In order to confirm **14** can bind to AβOs, the inhibition of Aβ42 oligomerization was performed and assessed using Western blot analysis as described in the literature.[29] As shown in Figure 5A, Aβ42 formed oligomers under the reported protocol as demonstrated by transmission electron microscopy (TEM) analysis. After incubation in Ham's F-12 medium for 4 h at 37 °C, higher order species of AβOs were formed (Figure 5B, lane 2). Notably, both **1** and **14** inhibited the oligomerization of Aβ42 (Figure 5B, lanes 3 and 4), which demonstrates their direct binding to Aβ42. This further confirms that the addition of spacer in **14** does not affect its binding interactions with Aβ42. Next, immunocytochemistry studies were conducted to confirm the interactions of **14** with the CM/LR taking advantage of the intrinsic fluorescence of **14**. As shown in Figure 5C, **14** was detected primarily on the cell membrane of MC65 cells (yellow puncta)

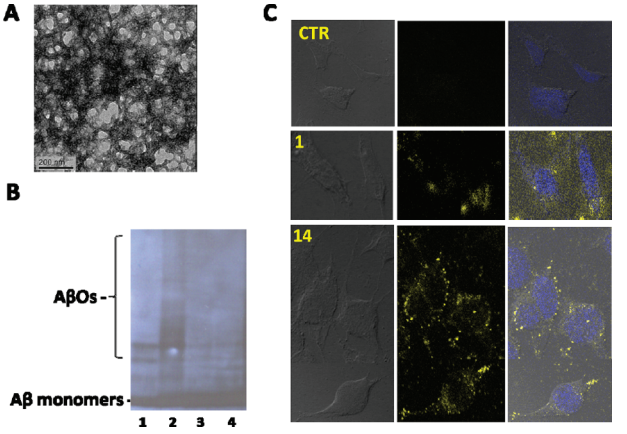

Figure 5. Binding interactions of **14** with Aβ42 and the CM/LR of MC65 cells. (A) TEM image of AβOs. (B) Aβ42 (5 μM) was incubated with or without compounds (20 μM), and then samples were analyzed by Western blot using 6E10 antibody. Lane 1 - Aβ42 without incubation; Lane 2 - Aβ42 with incubation; Lane 3 - Aβ42 with **1**; Lane 4 - Aβ42 with **14**. (C) MC65 cells were treated and imaged as in Figure 4. Left panel - differential interference contrast (DIC) images of MC65 cells; central panel - fluorescence of **14** and **1**; right panel - overlay of left and central panels plus DAPI staining of nucleus.

and inside of MC65 cells as well (bottom panel). **1** was detected inside of MC65 cells but not on the cell membrane (middle panel). The results demonstrate that **14** can directly interact with CM/LR of MC65 cells and anchor the ligand primarily to the CM/LR. Given the fact that Aβ aggregates on the cell surface,[17−19] the anchorage of **14** to CM/LR may increase its target accessibility and consequently increase its potency. Collectively, these results support our design rationale of using BMAOIs to cotarget AβOs and CM/LR.

Protective Effects of 14 on AβOs-Induced Cytotoxicity in MC65 Cells and Differentiated Human Neuroblastoma SH-SY5Y Cells. The production of intracellular AβOs has been suggested to be the major factor leading to cytotoxicity in MC65 cells.[39] Therefore, to test whether the suppression of AβOs formation by **14** correlate with functional activities, **14** was further evaluated for its protective effects on MC65 cell viability upon removal of TC. As shown in Figure 6A, **1** and **14** exhibited no toxic effects at tested concentrations in the presence of TC. Upon removal of TC, MC65 cell viability was significantly decreased and **14** protected MC65 cell survival in a dose-dependent manner with nearly full rescue at 16 μM. **1** only exhibited minimal protective effects on MC65 cell viability consistent with reported results.[39] **8** and **12** exhibited no protective effects under these conditions (data not shown) which further suggests the importance of spacer length and attachment position on their activities. Together with the results from Western blot and immunocytochemistry assays, these data suggest that the localization of **14** to the CM/LR may increase **14**'s target accessibility and produce a more profound inhibition of the formation of AβOs and elevate the survival of MC65 cells. To further verify whether **14** can protect cells from extracellular AβOs-induced cytotoxicity, all *trans*-retinoic acid differentiated human SH-SY5Y cells were employed. As shown in Figure 6B, freshly prepared AβOs (1 μM) from Aβ42 significantly decreased SH-SY5Y cell viability (~40% decrease). Notably, **14** completely restored the cell viability at all of the tested concentrations. On the other hand, **1** only exhibited moderate protective activities at 2, 4, and 8 μM concentrations

but not at 16 μM. This may be due to its toxic effect on SH-SY5Y cells at this concentration since **1** has been reported to have cytotoxicity on SH-SY5Y cells at higher concentrations.[44] These results suggest that **14** can protect cells from both intracellular and extracellular AβOs-induced cytotoxicity, while **1** only exhibits protective activity toward extracellular AβOs-induced cytotoxicity even though it can cross the cell membrane under these experimental conditions. This may further indicate that while both **1** and **14** can bind to AβOs, CM/LR anchorage of **14** can increase its accessibility to intracellular target AβOs. Since CM/LR are crucial for many aspects of cell signaling and functions, **14** was further evaluated for its potential cytotoxicity in mouse spleen and natural killer (NK) cells. **14** showed minimal cytotoxic effects in mouse spleen (Figure 6C) and no cytotoxic effects in NK cells (Figure 6D). This suggests that localization of BMAOIs to the CM/LR will not affect the normal cellular functions. Taken together, it is clear that **14** is more active than **1** in inhibiting the production of AβOs and in protecting cells from the in situ AβOs-induced cytotoxicity.

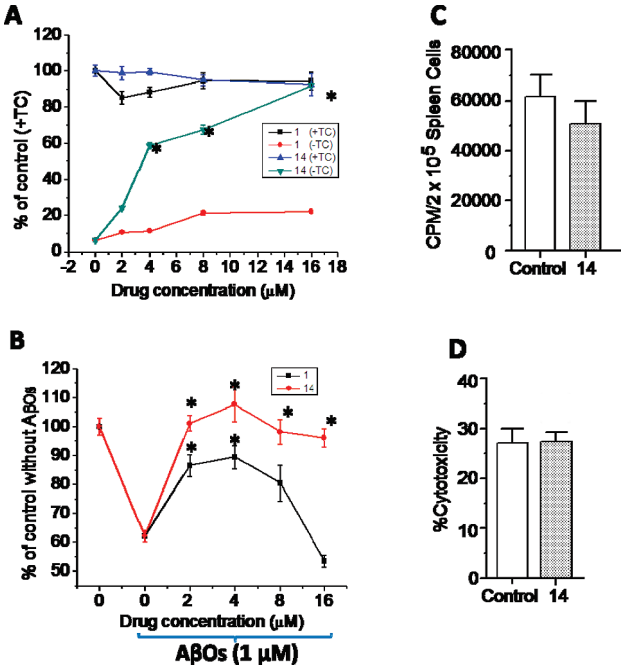

Figure 6. Protective effects of **14**. (A) MC65 cells were treated with **1** or **14** at indicated concentrations under +TC or −TC conditions for 72 h. Cell viability was assayed by MTS assay. Data were expressed as mean percentage viability (n = 6) with parallel +TC cultures set at 100% viability. Error bars represent SEM. (B) All-*trans*-retinoic acid differentiated SH-SY5Y cells were treated with AβOs (1 μM) in the presence or absence of test compounds at indicated concentrations for 48 h. Cell viability was assayed by MTS assay. Data were expressed as mean percentage viability (n = 6) with cultures without AβOs set at 100% viability. Error bars represent SEM. (C) Effects of 14 (10 μM) on anti-CD3 antibody mediated splenocyte proliferation. (D) Effects of 14 (10 μM) on IL-2 augmented NK cell activity in vitro. The experiments were performed as described in the Experimental Section. Data were presented as mean (n = 4) ± SEM. *P < 0.05 indicates significant differences from control group (without TC in A and without AβOs in B) analyzed by one-way ANOVA.

Antioxidant Activity of 14. One of the BMAOIs design goals is to reduce oxidative stress that potentially contributes to the development of AD. Furthermore, oxidative stress has been indicated as one potential effector to impart neurotoxicity upon the accumulation of intracellular AβOs in MC65 cells.[40] Therefore, we decided to further evaluate the antioxidant activity of **14** in MC65 cells. Despite the availability of several chemical antioxidation assays, the ability to predict and correlate these chemical assays with in vivo activity is questionable. In contrast, a cellular antioxidation assay may provide a more biologically relevant system that best addresses the permeability, distribution, and metabolism issues to evaluate potential antioxidant properties. Recently, a dichlorofluorescein diacetate (DCFH-DA) based cellular antioxidant assay has been established and widely used for this purpose.[45] We therefore adopted this DCFH-DA assay in MC65 cells to evaluate the antioxidant effects of **14** and **1**. As shown in Figure 7A, upon TC removal, intracellular oxidative stress, as measured by fluorescence intensity, is significantly increased compared to normal growing MC65 cells in the presence of TC. Notably, both **14** and **1** suppressed the intracellular oxidative stress in a dose-depndent manner. These results may indicate that the curcumin moiety in **14** is responsible for its antioxidant activities. Although **1** exhibited antioxidant activities in this cellular model, it did not protect MC65 cell survival (Figure 6A). To compare whether other antioxidants can protect MC65 cells from AβOs-induced cytotoxicity, *N*-acetylcysteine (NAC) and trolox (6-hydroxy-2,5,7,8-tetramethyl chroman-2-carboxylic acid), an analogue of vitamin E, were tested in MC65 cells. As shown in Figure 7B, trolox (32 μM) completely

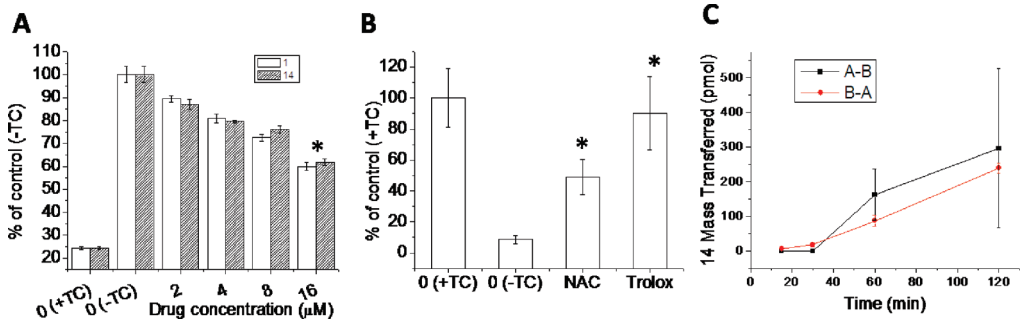

Figure 7. Antioxidant effects and Caco-2 permeability of **14**. (A) MC65 cells were treated with **1** or **14** at indicated concentrations under +TC or −TC conditions for 24 h, and then DCFH-DA (25 μM) was loaded and fluorescence intensity was analyzed at 485 nm (excitation) and 530 nm (emission). Data were presented as mean percentage of fluorescence intensity (n = 5) with parallel −TC cultures set at 100%. Error bars represent SEM. (B) MC65 protection was performed as described in Figure 6A with NAC (8 mM) or trolox (32 μM) (n = 5). (C) Caco-2 cells were plated on transwell filters. Test compounds (10 μM) were added to either the apical or basolateral side, and then samples were analyzed by HPLC to determine flux (A-B: apical-to-basolateral; B-A: basolateral-to-apical) at indicated time points. Data were presented as mean (n = 3) ± SEM. *P < 0.05 indicates significant differences from control group (−TC) analyzed by one-way ANOVA.

rescued MC65 cells from AβOs-induced cytotoxicity, while NAC (8 mM) rescued MC65 cells by 48% consistent with reported results.[40] Given the fact that NAC is mainly a hydrogen peroxide scavenger while trolox, a chain-breaking antioxidant, is particularly effective against lipid peroxidation within the cell membrane,[46] these results may indicate lipid peroxidation within the cell membrane as a major contributor underlying the mechanism of AβOs-induced cytotoxicity in MC65 cells, which is consistent with the results from Woltjer et al.[47] The discrepancy of **1** and the other two antioxidants in MC65 cell-protection may suggest that **1** either cannot reach the targets or only partially suppress lipid peroxidation in MC65 cells. Together with the results from Western blot analysis, immunocytochemistry, and cell protection, the results of antioxidation assay further suggest that **14** can retain the antioxidant property of **1** while exhibiting superior capability to reach intracellular AβOs by interacting with the CM/LR, thus efficiently reducing the formation of AβOs and ultimately exhibiting better overall protective activities in these cells when compared to **1**. This further supports the idea that our BMAOIs strategy has the potential to provide clinically efficient multifunctional agents for treatment of AD.

Assessment of Permeability and P-Glycoprotein Using Caco-2 Cell Model. Because of the adverse effects of AD in the central nervous system, effective drug candidates need to cross the blood−brain barrier (BBB). To test whether **14** has the potential to reach the brain, we determined its permeability and transport directionality using the Caco-2 model.[48] Although the Caco-2 cell monolayer model is derived from the colon rather than the brain, this model expresses efflux transporters such as P-glycoprotein which are also expressed at the BBB. The Caco-2 model does not predict BBB penetration as well as other models, such as PAMPA-BLM, ECV/C6, or hCMEC/D3;[49−51] however, this model can provide early screening regarding the transcellular diffusional permeability and directional efflux transport across the BBB.[52] As shown in Figure 7C, the apical-to-basolateral and basolateral-to-apical permeabilities of **14** were $7.1 \pm 4.6 \times 10^{-6}$ and $4.7 \pm 0.5 \times 10^{-6}$ cm/s, respectively. Thus, **14** exhibits good bidirectional permeability in Caco-2 cells. In contrast, we were unable to detect transport of **1**, likely due to its extensive metabolism by glutathione-*S*-transferase enzymes.[53] This further indicates that CM/LR anchorage of **14** can improve its metabolic stability compared to **1**. The permeability directional ratio (efflux ratio) for **14** is 0.63, so it does not appear to be a substrate for BBB efflux transporters such as P-glycoprotein, since the efflux ratio is < 2.[54] These data further support the potential of **14** as a new lead to develop effective AD treatment agents. Furthermore, in vivo studies have demonstrated the ability of **1** to cross the BBB,[29,55,56] so **14** is anticipated to be able to cross the BBB and the results from Caco-2 assay also supports this notion. Future in vivo studies will assess the BBB permeability more directly, and studies are being undertaken in our laboratory to evaluate **14**'s BBB permeability in mice.

Conclusion

In summary, a series of BMAOIs containing **1** and **2** were designed and synthesized to cotarget AβOs, oxidative stress, and CM/LR. Biological characterization from in vitro assays established that spacer length and the spacer attachment position on **1** are important structural determinants for their biological activities. Among the designed BMAOIs, **14** with a 21-atom-spacer was identified to localize to the CM/LR of MC65 cells, to efficiently inhibit the production of intracellular AβOs in MC65 cells, and to protect MC65 cells and differentiated SH-SY5Y cells from the cytotoxicity of AβOs. Furthermore, **14** exhibited antioxidant properties and demonstrated potential to cross the BBB using a Caco-2 model. These results strongly encourage further optimization of **14** as a new hit to develop more potent BMAOIs. These results may also help validate BMAOIs strategy as a novel design strategy to provide effective multifunctional ligands as potential AD treatment agents.

Experimental Section

Chemistry. Reagents and solvents were obtained from commercial suppliers and used as received unless otherwise indicated. All reactions were carried out under inert atmosphere (N_2) unless otherwise noted. Reactions were monitored by thin-layer chromatography (TLC) (precoated silica gel 60 F_{254} plates, EMD Chemicals) and visualized with UV light or by treatment with phosphomolybdic acid (PMA). Flash chromatography was performed on silica gel (200−300 mesh, Fisher Scientific) using solvents as indicated. ^{1}HNMR and ^{13}CNMR spectra were routinely recorded on Bruker ARX 400 spectrometer. The NMR solvent used was $CDCl_3$ or DMSO-d_6 as indicated. Tetramethylsilane (TMS) was used as the internal standard. The purity of target BMAOIs was determined by HPLC using a Varian 100-5 C18 250 × 4.6 mm column with UV detection (288 nm) (40% acetonitrile/60% methanol/0.1% trifluoroacetic acid (TFA) and 38% acetonitrile/62% H_2O/2% acetic acid, pH 3.0 two solvent systems) to be ≥95%.

4-Methoxy-3-propargyloxy-benzaldehyde (18). A mixture of vanillin **17** (0.76 g, 4.90 mmol), K_2CO_3 (1.37 g, 9.90 mmol), and propargyl bromide (1.19 g, 6.90 mmol) in DMF (30 mL) was refluxed at 80 °C for 1 h. Reaction mixture was cooled to 0 °C in an ice bath and filtered through a short bed of Celite. Ethyl acetate (50 mL) was added and the mixture was washed with 1 N HCl (20 mL), extracted with ethyl acetate (100 mL). The organic phase was combined and washed with brine and dried over anhydrous Na_2SO_4. After filtration, solvent was removed under reduced pressure and the crude residue was purified by flash chromatography (hexane/ethyl acetate: 8/2) to afford **18** as white solid (0.74 g, 80%). ^{1}HNMR (400 MHz, $CDCl_3$) δ 2.57 (t, 1H), 3.94 (s, 3H), 4.85−4.86 (d, J = 2.44 Hz, 2H), 7.13−7.15 (d, J = 8.16 Hz, 1H), 7.43−7.47 (m, 2H), 9.87 (s, 1H); ^{13}CNMR (100 MHz, $CDCl_3$) δ 56.06, 56.65, 109.58, 112.71, 126.21, 131.00, 150.11, 152.17, 190.85.

5-Hydroxy-1-(4-hydroxy-3-methoxy-phenyl)-7-(3-methoxy-4-propargyloxy-phenyl)-hepta-1,4,6-trien-3-one (20). Compound **20** was prepared by Pabon reaction following the reported procedure[57] from 2,4-pentane-dione and **17**. ^{1}HNMR (400 MHz, $CDCl_3$) δ 2.53−2.54 (t, J = 4.84, 3H), 3.92−3.93 (d, J = 6.2 Hz, 6H), 4.79−4.80 (d, J = 2.32 Hz, 2H), 5.81 (s, 1H), 6.45−6.51 (m, 2H), 6.91−6.93 (d, J = 8.2 Hz, 1H), 7.04 (s, 2H), 7.08−7.12 (m, 3H), 7.57−7.61 (d, J = 15.72 Hz, 2H); ^{13}CNMR (100 MHz, $CDCl_3$) δ 26.78, 55.97, 56.67, 60.41, 101.28, 109.70−129.31, 140.08−149.83, 182.83, 183.68.

3-Propargyl-pentane-2,4-dione (22). The mixture of propargyl bromide (0.32 g, 2.70 mmol), K_2CO_3 (2.22 g, 16.10 mmol), and 2,4-pentane-dione (1.34 g, 13.40 mmol) in acetone (30 mL) was stirred for 24 h at 60 °C. After filtration and removal of solvent under reduced pressure, the crude residue was purified by flash chromatography (hexane) to give **22** as colorless liquid (0.30 g, 69%). ^{1}HNMR (400 MHz, $CDCl_3$) δ 2.03−2.04 (t, J = 5.28 Hz, 1H), 2.22 (s, 3H), 2.25 (s, 3H), 2.68−2.71 (m, 2H), 3.84−3.87 (t, J = 15.08 Hz, 1H); ^{13}CNMR (100 MHz, $CDCl_3$) δ 14.45, 29.33, 29.41, 68.70, 70.79, 86.13, 202.18, 202.63.

1,7-Bis-(4-hydroxy-3-methoxy-phenyl)-4-propargyl-hepta-1,6-diene-3,5-dione (23). Compound **22** (0.81 g, 5.90 mmol) was reacted with boric anhydride (0.29 g, 4.10 mmol), **17** (0.18 g, 11.70 mmol), tributylborate (5.39 g, 23.40 mmol), and *n*-butylamine (0.64 g, 8.80 mmol) following a reported procedure[57] to afford **23** as a yellow solid (0.50 g, 21%). ^{1}HNMR (400 MHz, $CDCl_3$) δ 2.14−2.16 (t, J = 5.08 Hz, 1H), 2.89−2.92 (m, 2H), 3.91 (s, 3H), 3.95 (s, 3H), 6.68−6.72 (d, J = 15.8 Hz, 1H), 6.90−7.26 (m, 8H), 7.56−7.74 (m, 2H); ^{13}CNMR (100 MHz, $CDCl_3$) δ 16.27, 56.03, 69.61, 70.57, 82.66, 106.24, 109.83−127.97, 142.43−148.87, 182.68, 193.34.

Cholesteryl-3-acetic Acid (25). 25 was prepared following the reported procedure[33] from cholesterol as a white solid. ^{1}HNMR (400 MHz, $CDCl_3$) δ 0.67 (s, 3H), 0.85−0.87 (dd, J = 6.64 Hz, 1.68 Hz, 6H), 0.90−0.92 (d, J = 6.52 Hz, 3H), 1.00−2.40 (31H), 3.26−3.34 (m, 1H), 4.14 (s, 2H), 5.36−5.37 (t, J = 5.2 Hz, 1H); ^{13}CNMR (100 MHz, $CDCl_3$) δ 11.86−42.33, 50.13, 56.17, 56.74, 65.20, 80.45, 122.40, 139.98, 173.89.

Procedure A. Preparation of 3-Amino-*N*-(4-azido-butyl)-propionamide (28). To a mixture of Boc-protected β-alanine (1.00 mmol) and hydroxybenzotriazole (HOBt) (1.50 mmol) in CH_2Cl_2 (10 mL) was added 1-ethyl-3-(3-dimethylaminopropyl)-carbodiimide (EDC) (1.50 mmol) at 0 °C. The reaction mixture was stirred for 1 h at room temperature. Then, a solution of TFA salt of 4-azido-butylamine 26 (2.00 mmol) and Et_3N (3.00 mmol) in CH_2Cl_2 (5 mL) was added to the reaction mixture at 0 °C. The reaction mixture was then stirred overnight at room temperature. The reaction mixture was washed with H_2O, $NaHCO_3$, and brine. The organic phase was dried over anhydrous Na_2SO_4 and the solvent was removed under reduced pressure. The crude residue was purified by flash chromatography (MeOH/CH_2Cl_2: 3/97) and deprotected using TFA/CH_2Cl_2 (0.5 mL per 1 mmol of Boc-protected azido product) to afford **28** as a colorless viscous liquid. ^{1}HNMR (400 MHz, DMSO-d_6) δ 1.41−1.61 (m, 4H), 2.50−2.51 (m, 2H), 2.89−2.98 (m, 2H), 3.01−3.09 (m, 2H), 3.31−3.34 (t, J = 13.32, 2H); ^{13}CNMR (100 MHz, DMSO-d_6) δ 25.74, 26.19, 32.01, 35.22, 37.90, 48.51, 50.33, 169.16.

3-Amino-*N*-(6-azido-hexyl)-propionamide (29). 6-Azido-hexylamine **27** (2.00 mmol) was reacted with Boc-protected β-alanine (1.00 mmol) following Procedure A to give **29**. ^{1}HNMR (400 MHz, DMSO-d_6) δ 1.20−1.46 (m, 8H), 2.40−2.44 (m, 2H), 2.84−2.87 (m, 2H), 2.93−2.98 (m, 2H), 3.21−3.24 (t, J = 13.64, 2H); ^{13}CNMR (100 MHz, DMSO- d6) δ 25.80, 25.89, 28.12, 28.78, 31.98, 35.25, 38.37, 50.55, 169.07.

3-Amino-*N*-[2-(4-azido-butylcarbamoyl)-ethyl]-propionamide (30). Compound **28** (2.00 mmol) was reacted with Boc-protected β-alanine (1.00 mmol) following Procedure A to give **30**. ^{1}HNMR (400 MHz, DMSO-d_6) δ 1.42−1.54 (m, 4H), 2.24−2.28 (t, J = 14.2 Hz, 2H), 2.45−2.50 (m, 4H), 2.9−3.03 (m, 5H), 3.21−3.32 (m, 4H); ^{13}CNMR (100 MHz, DMSO-d_6) δ 25.71, 26.18, 26.25, 31.19, 32.03, 34.53, 35.19, 35.23, 35.39, 37.81, 38.83, 50.33, 51.69, 54.88,169.22, 170.15.

3-Amino-*N*-[2-(6-azido-hexylcarbamoyl)-ethyl]-propionamide (31). Compound **29** (2.00 mmol) was reacted with Boc-protected β-alanine (1.00 mmol) following Procedure A to give **31**. ^{1}HNMR (400 MHz, DMSO-d_6) δ 1.22−1.54 (m, 10H), 2.22−2.25 (t, J = 14.12 Hz, 2H), 2.9−3.1 (m, 6H), 3.23−3.27 (m, 2H), 3.31−3.35 (t, 2H); ^{13}CNMR (100 MHz, DMSO-d_6) δ 25.80, 25.88, 28.13, 28.87, 32.03, 35.18, 35.24,35.39, 38.31, 38.84, 50.54, 54.89,169.31, 170.04.

Procedure B. Preparation of 32. The mixture of compound **25** (1.00 mmol), EDC (1.50 mmol), and HOBt (1.50 mmol) in CH_2Cl_2 (10 mL) was stirred for 1 h at room temperature. To this solution was added a solution of **26** (3.00 mmoL) and Et_3N (4.00 mmol) in CH_2Cl_2 (5 mL) at 0 °C. The reaction mixture was then stirred overnight at room temperature. After filtration through a short bed of Celite, the organic phase was washed with H_2O, $NaHCO_3$, and brine, followed by drying over anhydrous Na_2SO_4. Organic solvent was removed under reduced pressure and the crude product was purified by flash chromatography (MeOH/CH_2Cl_2: 3/97) to afford **32**. ^{1}HNMR (400 MHz, $CDCl_3$) δ 0.61 (s, 3H), 0.78−0.80 (dd, J = 4.96 Hz, 1.6 Hz, 6H), 0.81−0.83 (d, J = 9.44 Hz, 3H), 0.85−2.30 (m, 37H), 3.15−3.26 (m, 3H), 3.89 (s, 2H), 5.28−5.29 (t, J = 5.16 Hz, 1H); ^{13}CNMR (100 MHz, $CDCl_3$) δ 10.84−41.32, 49.12, 50.06, 55.16, 55.73, 66.58, 79.22, 121.31, 139.04, 169.30.

Preparation of 33. Compound **25** (1.00 mmol) was reacted with **27** (3.00 mmol) following Procedure B to give **33**. ^{1}HNMR (400 MHz, $CDCl_3$) δ 0.61 (s, 3H), 0.78−0.80 (dd, J = 4.88 Hz, 1.72 Hz, 6H), 0.83−0.85 (d, J = 9.44 Hz, 3H), 0.94−2.30 (41H), 3.14−3.23 (m, 3H), 3.89 (s, 2H), 5.28−5.29 (t, J = 5.24 Hz, 1H); ^{13}CNMR (100 MHz, $CDCl_3$) δ 10.85−41.32, 49.13, 50.35, 55.16, 55.73, 66.62, 79.22, 121.30, 139.07, 169.18.

Preparation of 34. Compound **25** (1.00 mmol) was reacted with **28** (3.00 mmol) following Procedure B to give **34**. ^{1}HNMR (400 MHz, $CDCl_3$) δ 0.60 (s, 3H), 0.85−0.87 (dd, J = 4.92 Hz, 1.68 Hz, 6H), 0.90−0.92 (d, J = 6.48 Hz, 3H), 1.00−2.39 (39H), 3.09−3.18 (m, 1H), 3.20−3.25 (m, 4H), 3.48−3.53 (m, 2H), 3.88 (s, 2H), 5.27−5.29 (t, J = 5.04 Hz, 1H); ^{13}CNMR (100 MHz, $CDCl_3$) δ 10.84−41.32, 49.14, 50.03, 55.16, 55.74, 66.50, 79.29, 121.23, 139.12, 169.86, 169.99.

Preparation of 35. Compound **25** (1.00 mmol) was reacted with **29** (3.00 mmol) following Procedure B to give **35**. ^{1}HNMR (400 MHz, $CDCl_3$) δ 0.67 (s, 3H), 0.85−0.87 (dd, J = 4.92 Hz, 1.68 Hz, 6H), 0.90−0.92 (d, J = 6.48 Hz, 3H), 1.00−2.43 (43H), 3.16−3.27 (m, 5H), 3.57−3.60 (m, 2H), 3.95 (s, 2H), 5.34−5.35 (t, J = 5.04 Hz, 1H); ^{13}CNMR (100 MHz, $CDCl_3$) δ 11.84−42.32, 50.15, 51.33, 56.16, 56.74, 67.53, 80.29, 122.21, 140.12, 170.81, 170.87.

Preparation of 36. Compound **25** (1.00 mmol) was reacted with **30** (3.00 mmol) following Procedure B to give **36**. ^{1}HNMR (400 MHz, $CDCl_3$) δ 0.67 (s, 3H), 0.85−0.87 (dd, J = 4.92 Hz, 1.68 Hz, 6H), 0.90−0.92 (d, J = 6.48 Hz, 3H), 1.00−2.58 (41H), 3.17−3.35 (m, 2H), 3.51−3.59 (m, 3H), 3.70 (s, 2H), 3.96 (s, 2H), 5.35−5.36 (t, J = 3.28 Hz, 1H); ^{13}CNMR (100 MHz, $CDCl_3$) δ 10.84−41.31, 49.12, 50.00, 50.79, 55.15, 55.73, 66.56, 79.29, 121.24, 139.09, 169.45, 171.66.

Preparation of 37. Compound **25** (1.00 mmol) was reacted with **31** (3.00 mmol) following Procedure B to give **37**. ^{1}HNMR (400 MHz, $CDCl_3$) δ 0.67 (s, 3H), 0.85−0.87 (dd, J = 4.88 Hz, 1.72 Hz, 6H), 0.90−0.92 (d, J = 6.52 Hz, 3H), 1.00−2.58 (45H), 3.16−3.26 (m, 1H), 3.50−3.59 (m, 3H), 3.95−3.96 (d, J = 3.56 Hz, 2H), 5.34−5.36 (t, J = 5.76 Hz, 1H); ^{13}CNMR (100 MHz, $CDCl_3$) δ 11.87−42.33, 50.15, 51.81, 51.85, 56.17, 56.75, 67.59, 80.29, 122.20, 140.12, 170.47, 170.73, 171.09.

Procedure C. Preparation of BMAOI 3. To the solution of compounds **32** (1 equiv) and compound **20** (2 equiv) in THF/H_2O (5 mL, 1:1) was added sodium ascorbate (0.04 equiv) and $CuSO_4$ (0.02 equiv) at room temperature. The reaction mixture was stirred for 24 h at 65 °C. The solvent was removed under reduced pressure and CH_2Cl_2 (5 mL) was added. The organic layer was washed with H_2O and brine, and then dried over anhydrous Na_2SO_4. After filtration and removal of the solvent under reduced pressure, the crude residue was purified by flash chromatography (MeOH/CH_2Cl_2: 5/95) to give BMAOI **3** as a yellow solid. ^{1}HNMR (400 MHz, $CDCl_3$) δ 0.67 (s, 3H), 0.85−0.87 (dd, J = 4.92 Hz, 1.64 Hz, 6H), 0.90−0.91 (d, J = 6.48 Hz, 3H), 0.99−2.34 (35H), 3.15−3.21 (m, 1H), 3.30−3.35 (m, 2H), 3.91 (s, 2H), 3.94 (s, 3H), 3.95 (s, 3H), 4.37−4.40 (t, J = 14.08 Hz, 2H), 5.32 (s, 2H), 5.32−5.34 (m, 1H), 6.46−6.50 (d, 2H), 6.92−6.94 (d, 1H), 7.05−7.13 (m, 5H), 7.56 (d, 1H), 7.60 (d, 1H), 7.65 (s, 1H); ^{13}CNMR (100 MHz, $CDCl_3$) δ 11.86−42.32, 49.86−50.11, 55.97−56.72, 63.10, 67.50, 80.21, 101.24, 109.66−128.85, 140.06−149.67, 170.49, 182.92−183.58.

Preparation of BMAOI 9. Compounds **32** (1 equiv) was reacted with compound **23** (2 equiv) in THF/H_2O (5 mL, 1:1) following Procedure C to give BMAOI 9. ^{1}HNMR (400 MHz, $CDCl_3$) δ 0.67 (s, 3H), 0.85−0.87 (dd, J = 4.88 Hz, 1.72 Hz, 6H), 0.90−0.92 (d, J = 6.52 Hz, 3H), 0.99−2.35 (35H), 3.16−3.28

(m, 3H), 3.39−3.34 (m, 2H), 3.90 (s, 3H), 3.93 (s, 3H), 3.94 (s, 2H), 4.27−4.31 (t, J = 14 Hz, 2H), 5.33−5.35 (t, J = 5.08 Hz, 1H), 6.64−6.68 (d, 2H), 6.88−6.91 (m, 3H), 6.92−7.09 (m, 4H), 7.58−7.62 (d, 1H), 7.68−7.72 (d, 1H); ^{13}CNMR (100 MHz, $CDCl_3$) δ 11.86−42.33, 49.67−50.12, 56.04−56.73, 63.07, 67.48, 80.22, 108.87, 109.83−128.88, 140.09−149.67, 170.51, 182.12, 194.47.

Preparation of BMAOI 4. Compounds **33** (1 equiv) was reacted with compound **20** (2 equiv) in THF/H_2O (5 mL, 1:1) following Procedure C to give BMAOI **4**. ^{1}HNMR (400 MHz, $CDCl_3$) δ 0.67 (s, 3H), 0.85−0.87 (dd, J = 4.88 Hz, 1.72 Hz, 6H), 0.90−0.91 (d, J = 6.52 Hz, 3H), 1.00−2.34 (39H), 3.21−3.29 (m, 3H), 3.91 (s, 2H), 3.94 (s, 3H), 3.95 (s, 3H), 4.31−4.35 (t, J = 14.36 Hz, 2H), 5.33 (s, 2H), 5.33 (t, 1H), 6.46 (d, 1H), 6.50 (d, 1H), 6.92−6.94 (d, 1H), 7.05−7.13 (m,5H), 7.56−7.57 (d, 1H), 7.60−7.61 (d,1H), 7.62 (s, 1H); ^{13}CNMR (100 MHz, $CDCl_3$) δ 11.86−42.33, 50.11−50.32, 55.98−56.72, 63.10, 67.59, 80.22, 101.24, 109.66−128.85, 140.06−149.67, 170.26, 182.92−183.56.

Preparation of BMAOI 10. Compounds **33** (1 equiv) was reacted with compound **23** (2 equiv) in THF/H_2O (5 mL, 1:1) following Procedure C to give BMAOI 10. ^{1}HNMR (400 MHz, $CDCl_3$) δ 0.60 (s, 3H), 0.85−0.87 (dd, J = 4.88 Hz, 1.72 Hz, 6H), 0.90−0.91 (d, J = 6.52 Hz, 3H), 0.99−2.44 (39H), 3.07−3.18 (m, 3H), 3.31−3.33 (m, 4H), 3.82 (s, 3H), 3.84 (s, 3H), 3.89 (s, 2H), 4.16−4.18 (t, J = 11.92 Hz, 2H), 5.27−5.28 (t, J = 5.16 Hz, 1H), 6.58−6.62 (d, 1H), 6.79−6.83 (m, 2H), 6.92−7.00 (m, 4H), 7.24 (s, 1H), 7.49−7.53 (d, 1H), 7.60−7.64 (d, 1H); ^{13}CNMR (100 MHz, $CDCl_3$) δ 10.84−41.31, 49.11−50.15, 55.01−55.71, 62.90, 66.55, 79.24, 108.87, 109.92−128.88, 140.09−149.67, 170.26, 182.12, 193.57.

Preparation of BMAOI 5. Compounds **34** (1 equiv) was reacted with compound **20** (2 equivalent) in THF/H_2O (5 mL, 1:1) following Procedure C to give BMAOI 5. ^{1}HNMR (400 MHz, $CDCl_3$) δ 0.66 (s, 3H), 0.84−0.87 (dd, J = 4.96 Hz, 1.64 Hz, 6H), 0.89−0.91 (d, J = 6.48 Hz, 3H), 0.98−2.43 (37H), 3.15−3.2 (m, 1H), 3.26 (m, 2H), 3.55−3.57 (m, 4H), 3.91 (s, 2H), 3.93 (s, 6H), 4.36 (t, 2H), 5.33 (s, 2H), 5.33 (t, 1H), 6.48 (d, 2H), 6.93−6.19 (m,5H), 7.57−7.6610 (m, 3H); ^{13}CNMR (100 MHz, $CDCl_3$) δ 11.86−42.33, 49.86−50.14, 55.98−56.73, 63.02, 67.47, 80.30, 101.26, 109.79−128.93, 140.10−149.68, 170.09−171.23, 182.85−183.64.

Preparation of BMAOI 11. Compounds **34** (1 equiv) was reacted with compound **23** (2 equiv) in THF/H_2O (5 mL, 1:1) following Procedure C to give BMAOI **11**. ^{1}HNMR (400 MHz, $CDCl_3$) δ 0.67 (s, 3H), 0.85−0.87 (dd, J = 4.92 Hz, 1.68 Hz, 6H), 0.90−0.91 (d, J = 6.56 Hz, 3H), 0.99−2.44 (37H), 3.07−3.11 (m, 1H), 3.17−3.19 (m, 4H), 3.53−3.57 (m, 2H), 3.90 (s, 2H), 3.92 (s, 3H), 3.95 (s, 3H), 4.26−4.29 (t, J = 13.72 Hz, 2H), 5.33−5.34 (t, J = 2.88 Hz, 1H), 6.66−6.67 (d, 1H), 6.89−6.92 (m, 3H), 6.99−7.09 (m, 4H), 7.22 (s, 1H), 7.57−7.61 (d, 1H), 7.67−7.70 (d, 1H); ^{13}CNMR (100 MHz, $CDCl_3$) δ 11.87−42.34, 49.64−50.15, 56.07−56.75, 62.90, 67.49, 80.32, 108.87, 109.92−128.88, 140.09−149.67, 170.01−171.13, 182.12, 194.55.

Preparation of BMAOI 6. Compounds **35** (1 equiv) was reacted with compound **20** (2 equiv) in THF/H_2O (5 mL, 1:1) following Procedure C to give BMAOI **6**. ^{1}HNMR (400 MHz, $CDCl_3$) δ 0.67 (s, 3H), 0.85−0.87 (dd, J = 5 Hz, 1.6 Hz, 6H), 0.90−0.91 (d, J = 6.52 Hz, 3H), 0.99−2.44 (41H), 3.18−3.21 (m, 3H), 3.57−3.58 (m, 4H), 3.91 (s, 2H), 3.94 (s, 6H), 4.32−4.35 (t, J = 14.16 Hz, 2H), 5.33 (s, 2H), 5.33 (t, 1H), 6.46−6.47 (d, 1H), 6.50−6.51 (d, 1H), 6.92−6.94 (d,1H), 7.05−7.19 (m, 5H), 7.56−7.57 (d, 1H), 7.60−7.61 (d, 1H), 7.62 (s, 1H); ^{13}CNMR (100 MHz, $CDCl_3$) δ 11.86−42.33, 50.13−50.23, 55.98−56.74, 63.09, 67.52, 80.29, 101.25, 109.68−128.87, 140.09−149.67, 170.01−171.23, 182.95−183.55.

Preparation of BMAOI 12. Compounds **35** (1 equiv) was reacted with compound **23** (2 equiv) in THF/H_2O (5 mL, 1:1) following Procedure C to give BMAOI **12**. ^{1}HNMR (400 MHz, $CDCl_3$) δ 0.67 (s, 3H), 0.80−0.87 (dd, J = 4.92 Hz, 1.68, 6H), 0.90−0.91 (d, J = 6.64 Hz, 3H), 0.93−2.35 (41H), 3.03−3.22 (m, 3H), 3.38−3.40 (d, 1H), 3.53−3.67 (m, 3H), 3.90 (s, 2H), 3.94 (s, 3H), 3.96 (s, 3H), 4.22−4.27 (t, J = 14.88 Hz, 2H), 5.33−5.34 (t, J = 3.48, 1H), 6.65−6.69 (d, 1H), 6.89−6.91 (d, 2H), 6.98−7.09 (m, 4H), 7.20 (s, 1H), 7.55−7.59 (d, 1H), 7.67−7.71 (d, 1H); ^{13}CNMR (100 MHz, $CDCl_3$) δ 11.87−42.34, 50.14−50.19, 56.06−56.75, 63.06, 67.49, 80.33, 108.87, 109.88−128.88, 140.09−149.67, 170.01−171.23, 182.12, 194.62.

Preparation of BMAOI 7. Compounds **36** (1 equiv) was reacted with compound **20** (2 equiv) in THF/H_2O (5 mL, 1:1) following Procedure C to give BMAOI **7**. ^{1}HNMR (400 MHz, $CDCl_3$) δ 0.67 (s, 3H), 0.85−0.87 (d, J = 6.44 Hz, 6H), 0.90−0.91 (d, J = 6.48 Hz, 3H), 0.98−2.4 (39H), 3.20−3.28 (m, 3H), 3.52−3.56 (m, 4H), 3.91 (s, 2H), 3.94 (s, 3H), 3.96 (s, 3H), 4.36−4.39 (t, J = 13.56 Hz, 2H), 5.31 (s, 2H), 5.34 (t, 1H), 6.46−6.47 (d, 1H), 6.50−6.51 (d, 1H), 6.92−6.94 (d, 1H), 7.05−7.13 (m, 5H), 7.56−7.57 (d, 1H), 7.60−7.61 (d, 1H), 7.67 (s, 1H); ^{13}CNMR (100 MHz, $CDCl_3$) δ 11.86−42.33, 50.12−50.19, 55.98−56.73, 63.06, 67.57, 80.33, 101.26, 109.71−128.88, 140.09−149.67, 170.01−171.23, 182.85−183.64.

Preparation of BMAOI 13. Compounds **36** (1 equiv) was reacted with compound **23** (2 equiv) in THF/H_2O (5 mL, 1:1) following Procedure C to give BMAOI **13**. ^{1}HNMR (400 MHz, $CDCl_3$) δ 0.67 (s, 3H), 0.82−0.87 (dd, J = 4.88 Hz, 1.72 6H), 0.90−0.91 (d, J = 6.52 Hz, 3H), 0.93−2.4 (39H), 3.17−3.20 (m, 3H), 3.38−3.55 (m, 6H), 3.90 (s, 2H), 3.92 (s, 3H), 3.95 (s, 3H), 4.24−4.30 (t, J = 13.44 Hz, 2H), 5.33−5.34 (t, 1H), 6.65−6.67 (d, 1H), 6.69−6.71 (d, 1H), 6.89−6.91 (d, 1H), 7.00−7.09 (m, 5H), 7.57−7.61 (d, 1H), 7.67−7.71 (d, 1H), 7.63 (s, 1H); ^{13}CNMR (100 MHz, $CDCl_3$) δ 11.86−42.33, 50.12−50.19, 56.07−56.73, 63.06, 67.57, 80.33, 108.87, 109.71−128.88, 140.09−149.67, 170.01−171.23, 182.12, 193.57.

Preparation of BMAOI 8. Compounds **37** (1 equiv) was reacted with compound **20** (2 equiv) in THF/H_2O (5 mL, 1:1) following Procedure C to give BMAOI **8**. ^{1}HNMR (400 MHz, $CDCl_3$) δ 0.67 (s, 3H), 0.85−0.87 (dd, J = 4.92 Hz, 1.68 Hz, 6H), 0.90−0.91 (d, J = 6.52 Hz, 3H), 0.93−2.4 (43H), 3.17−3.22 (m, 3H), 3.48−3.56 (m, 4H), 3.89 (s, 2H), 3.94 (s, 3H), 3.96 (s, 3H), 4.36−4.39 (t, J = 12 Hz, 2H), 5.33 (s, 2H), 5.33 (t, 1H), 6.45−6.47 (d, 1H), 6.49−6.51 (d, 1H), 6.92−6.94 (d, 1H), 7.05−7.12 (m, 5H), 7.55−7.57 (d, 1H), 7.59−7.61 (d, 1H), 7.63 (s, 1H); ^{13}CNMR (100 MHz, $CDCl_3$) δ 11.86−42.32, 50.13−50.19, 55.98−56.73, 63.06, 67.57, 80.29, 101.26, 109.71−128.88, 140.09−149.67, 170.01−171.23, 182.85−183.64.

Preparation of BMAOI 14. Compounds **37** (1 equiv) was reacted with compound **23** (2 equiv) in THF/H_2O (5 mL, 1:1) following Procedure C to give BMAOI **14**. ^{1}HNMR (400 MHz, $CDCl_3$) δ 0.67 (s, 3H), 0.85−0.87 (dd, J = 4.88 Hz, 1.56 Hz 6H), 0.90−0.91 (d, J = 6.52 Hz, 3H), 0.93−2.4 (43H), 3.17−3.22 (m, 3H), 3.48−3.56 (m, 6H), 3.89 (s, 2H), 3.94 (s, 3H), 3.96 (s, 3H), 4.32−4.36 (t, J = 13.96 Hz, 2H), 5.33 (t, 1H), 6.45−6.47 (d, 1H), 6.49−6.51 (d, 1H), 6.92−6.94 (d, 1H), 7.05−7.12 (m, 5H), 7.56−7.57 (d, 1H), 7.59−7.61 (d, 1H), 7.63 (s, 1H); ^{13}CNMR (100 MHz, $CDCl_3$) δ 11.86−42.32, 50.13−50.19, 55.98−56.73, 63.06, 67.57, 80.29, 108.87, 109.71−128.88, 140.09−149.67, 170.01−171.23, 182.12, 193.57.

Biological Assays. Aβ42 was obtained from American Peptide, Inc. (Sunnyvale, CA). 6E10 antibody was obtained from Signet (Dedham, MA). A11 oligomer Rabbit polyclonal antibody, Alexa Fluor 568 donkey antirabbit IgG, Alexa 488 conjugated cholera toxin subunit B (CTX-B) were obtained from Invitrogen (CA, USA). 4′,6-Diamidino-2-phenylindole (DAPI) was obtained from Sigma-Aldrich (St. Louis, MO).

MC65 cells (kindly provided by Dr. George M. Martin at the University of Washington, Seattle) were cultured in Dulbecco's Modified Eagle's Medium (DMEM) (Life Technologies, Inc., Grand Island, NY) supplemented with 10% of heat-inactivated fetal bovine serum (FBS) (Hyclone, Logan, UT), 1 μg/mL TC, and 0.2 mg/mL G418 (Invitrogen) and maintained at 37 °C in a fully humidified atmosphere containing 5% CO_2. SH-SY5Y neuroblastoma cells were obtained from American Type

Culture Collection (ATCC) and were cultured in DMEM/Ham's F-12 (Invitrogen) supplemented with 10% FBS. ML60 cells were maintained in DMEM supplemented with 10% FBS, 0.2 mg/mL G418, and 25 μg/mL puromycin. All experiments were performed on 70% confluent growing cells unless otherwise indicated.

Western Blot Assay. MC65 cells were seeded in 6-well plates (1×10^6 cells/well). After incubation at 37 °C, 5% CO_2 for 24 h, the medium was replaced with fresh Opti-MEM (Invitrogen) and compounds in Opti-MEM (with or without TC) were added. After 24 h incubation, cells were collected on ice and centrifuged. Pellet was lysed by sonication in 1× lysis buffer (62.5 mM Tris base, pH 6.8, 2% SDS, 50 mM DTT, 10% glycerol, 0.1% bromphenol blue, and 5 mg/mL each chymostatin, leupeptin, aprotinin, pepstatin, and soybean trypsin inhibitor) and protein level was determined using Coomassie Protein Assay Reagent (Pierce, Rockford, IL). Equal amounts of protein (10 μg) were separated by SDS−PAGE on 10−20% tris-tricine gel (Bio-Rad) and transferred onto a PVDF membrane (Bio-Rad). The blots were blocked with 5% milk in TBS-Tween 20 (0.1%) at room temperature for 1 h and probed with primary 6E10 (1:2000) antibody overnight at 4 °C. The blots were then incubated with horseradish peroxidase-conjugated secondary antibody (1:2000. Kirkegaard & Perry, Gaithersburg, MD). The proteins were visualized by Western Blot Chemiluminescence Reagent (NEN Life Science Products, Boston, MA).

Immunocytochemistry Assay. MC65 cells were plated onto Lab-Tec chamber slides (1×10^4 cells/well). After 24 h incubation at 37 °C and 5% CO_2, Opti-MEM was added (with or without TC) and followed by test compounds. MC65 cells were incubated for 24 h. MC65 cells were rinsed 3x with PBS and incubated with Alexa 488-conjugated CTX-B (10 ug/mL) for 15 min on ice. After rinsing once with ice-cold PBS, cells were fixed for 30 min with 4% paraformaldehyde. MC65 cells were permeabilized for 30 min with 0.1% Triton X 100. Then MC65 cells were stained with A11 rabbit antibody followed by antirabbit Alexa 568 (1:500). Finally MC65 cells were treated with DAPI (5 μg/mL) and mounted with Vectashield Mounting Media. Cell fluorescence was analyzed by a Leica TCS-SP2 AOBS confocal laser scanning microscope equipped with blue diode, Argon, and 3 HeNe (lasers as well as a spectrophotometer based detection system with variable detector windows) using excitation lines at 355, 488, and 568 nm for DAPI, Alexa 488-conjugated CTX-B, and Alexa Fluor 568 donkey antirabbit IgG. Sequential scanning was conducted to ensure that there was no signal cross-talk between channels. Five different areas around the center were taken and the red puncta was averaged per cell.

For BMAOI **14** interaction with CM/LR immunocytochemistry assay, MC65 cells were incubated with 1 or 14 for 24 h, then fixed with 4% paraformaldehyde, and permeabilized with 0.1% Triton X100. MC65 cells were incubated with DAPI and mounted with Vectashield Mounting Media for confocal laser scanning using excitation lines at 355 and 494 nm. A series of optical sections (1024 × 1024 pixels) of 1.0 μm in thickness were taken through the cell depth for examined sample and projected as a single composite image by superimposition.

Aβ42 Oligomerization Inhibition Assay. An aliquot of Aβ42 (0.045 mg) was dissolved in 20 μL of DMSO and diluted in Ham's F-12 media without phenol red (Caisson's Laboratory, Inc., UT). Aβ42 (5 μM) was incubated with 1 or 14 (20 μM) in 37 °C water bath for 4 h. After incubation, the samples (50 μL) were spun down at 14000*g* for 10 min. The supernatant (20 μL) was mixed with an equal part of Tricine sample buffer without reducing agents (Bio-Rad). The unaggregated Aβ42 control was not incubated at 37 °C, and mixed with sample buffer (no centrifuging) and stored at −80 °C before it was electrophoresed. Samples (25 μL) were electrophoresed on a 10−20% Tris-Tricine gel, transferred to PVDF membrane, and blocked with 10% nonfat milk in PBS for 30 min. The blots were probed with 6E10 (1:2000) overnight at 4 °C, followed by horseradish peroxidase-conjugated secondary antibody (1:2000. Kirkegaard & Perry, Gaithersburg, MD). The proteins were visualized by Western Blot Chemiluminescence Reagent (NEN Life Science Products, Boston, MA).

Transmission Electron Microscope (TEM). Ten microliters of Aβ42 in Ham's F-12 (20 μM) were adsorbed onto 200-mesh carbon and formavar-coated grids (Electron Microscopy Sciences) for 20 min, washed for 1 min in distilled H_2O. The samples were negatively stained with 2% uranyl acetate (Electron Microscopy Sciences) for 5 min and washed for 1 min in distilled H_2O. The samples were air-dried overnight and viewed with a Jeol JEM-1230 TEM equipped with a Gatan UltraScan 4000SP 4K × 4K CCD camera (100 kV).

Cytotoxicity Assay in MC65 Cells. MC65 cells were seeded in 96-well plates (4×10^4 cells/well) at 37 °C, 5% CO_2 for 24 h. The medium was removed and washed with PBS twice. Opti-MEM and test compounds were added under +TC and −TC conditions. The plates were incubated at 37 °C, 5% CO_2 for 72 h, then 20 μL CellTiter 96 AQ_{ueous} One Solution (Promega, Madison, WI) were added to each well and the plates were incubated at 37 °C, 5% CO_2 for 2−4 h. The plates were read at 490 nm using FlexStation III plate reader (Molecular Devices). The blank with only test compounds in Opti-MEM was set up as background control for all of the tested concentrations. Each data point was averaged from six replicates and the experiments were independently repeated at least three times.

Cytotoxicity Assay in Differentiated SH-SY5Y Cells. SH-SY5Y cells were plated at 10 000 cells/well in type 1 collagen coated 96-well plates (Invitrogen) and were differentiated in Opti-MEM supplemented with 2% B-27 (Invitrogen) and 10 μM all-*trans*-retinoic acid for 7 days. The medium was removed and replaced with fresh maintenance medium. Freshly prepared Aβ42 oligomers in Ham's F-12 medium (1 μM) was added to cells for 48 h at 37 °C with or without test compounds. After treatment, 20 μL CellTiter 96 AQ_{ueous} One Solution (Promega, Madison, WI) were added to each well and the plates were incubated at 37 °C, 5% CO_2 for 2−4 h. The plates were read at 490 nm in FlexStation III plate reader (Molecular Devices). Each data point was averaged from six replicates and the experiments were independently repeated at least three times.

ML60 Cell Assay. Sandwich enzyme-linked immunoassays (ELISAs) for extracellular AβOs in ML60 cells were performed. ML60 cells (90% confluent) in 96-well plates were treated with test compounds (10 μM) at 37 °C, 5% CO_2 for 24 h. ML60 cells were centrifuged for 5 min at 6000*g*, and supernatant media was collected for AβOs measurement by ELISA. The capture antibody 21F12 (to Aβ residues 33−42) was used for capturing both monomeric and oligomeric Aβ42 species. The detecting antibody was biotinylated 21F12B, and the combination of 21F12 and biotinylated 21F12B allows the detection of only AβOs. The 21F12 mAbs were coated at 10 mg/mL into 96-well immunoassay plates (Costar) at room temperature overnight. The plates were then aspirated and blocked with 0.25% human serum albumin in PBS buffer for 1 h at room temperature. The plates were rehydrated with wash buffer (0.05% Tween 20 in TBS) before use. The samples were added to the plates and incubated at room temperature for 1 h. The plates were washed 3× with wash buffer between each step of the assay. The biotinylated 21F12B diluted to 0.5 mg/mL in casein assay buffer (0.25% casein, 0.05% Tween 20, pH 7.4, in PBS) was incubated in the wells for 1 h at room temperature. Avidin−horseradish peroxidase (Vector Laboratories), diluted 1:4000 in casein assay buffer, was added to the wells for 1 h at room temperature. The colorimetric substrate, Slow TMB-ELISA (Pierce), was added and allowed to react for 15 min, after which the enzymatic reaction was stopped with addition of 1 M H_2SO_4. Reaction product was quantified using plate reader by measuring the difference in absorbance at 450 and 650 nm.

Anti-CD3 Antibody Mediated Splenocyte Proliferation. A single spleen cell suspension from female B6C3F1 mice ($N = 4$) was prepared and resuspended in RPMI medium supplemented with FBS (10%), sodium bicarbonate (GIBCO), HEPES (GIBCO), L-glutamine, gentamicin, and 2-mercaptoethanol (0.00035%). The splenocytes (2×10^5/well) were cultured in the microtiter wells coated with anti-CD3 Ab (1 μg/mL; BD PharMingen) in the presence of 1 or 14 (10 μM) at 37 °C in 5% CO_2. Prior to harvest on day 3, the cells were pulsed with ^{3}H-thymidine for 18−24 h. The incorporation of ^{3}H-thymidine into the proliferating cells was used as the end point of the assay, and the data were expressed as CPM/2×10^5 cells.

IL-2 Augmented Natural Killer (NK) Cell Activity. To determine NK activity, single cell suspensions from female B6C3F1 mice ($N = 4$) were adjusted to 2.5×10^6 cells/mL in a 96-well U-bottom plate (0.1 mL/well) for each animal. Recombinant IL-2 (Chiron, Emeryville, CA) at a volume of 50 μL was added to each well so that the final concentration of IL-2 was 5000 IU/mL. The plates were cultured overnight in the presence of 1 or 14 (10 μM), and then assayed for NK cell activity using ^{51}Cr-labeled YAC-1 cells as the target cells. The ^{51}Cr-YAC-1 cells were added to each well of a 96-well plate to obtain E:T ratio of 50:1. The spontaneous release and the maximum release were determined by adding 0.1 mL of medium and Triton X-100 (0.1%) to each of 12 replicate wells containing the target cells, respectively. Following 4 h incubation, the plates were centrifuged, and 0.1 mL of the supernatant was removed from each well and the radioactivity counted. The mean percentage of cytotoxicity was determined.

DCFH-DA Antioxidation Assay. MC65 cells were seeded in 96-well plates (4×10^4 cells/well). After incubation at 37 °C, 5% CO_2 for 24 h, the medium was removed and washed with PBS. Opti-MEM and test compounds were added (+TC, −TC, and blank with only test compounds). MC65 cells were incubated at 37 °C, 5% CO_2 for 24 h. Then DCFH-DA in Opti-MEM was added to each well (final DCFH-DA concentration was 25 uM) and incubate at 37 °C, 5% CO_2 for 30 min. The medium was removed and replaced with fresh opti-MEM and plates were read for fluorescence intensity at 485 nm (excitation)/530 nm (emission) using FlexStation III plate reader (Molecular Devices).

Caco-2 Permeability Assay. Caco-2 cells (ATCC, Manassas, VA) were cultured in high-glucose DMEM supplemented with 10% FBS and used between passages 30−50. Caco-2 cells were plated on 12-well polyester transwell inserts (0.4 μM pore size) (Corning #3460) at a density of 80 000 cells/cm^2 and grown to 100% confluence (21 days). Filters were rinsed in Hank's balanced salt solution (HBSS) and test compounds (10 μM) were added to either the apical (0.5 mL) or basolateral (1.5 mL) side and incubated at 37 °C with shaking (100 rpm). Samples (200 μL) were removed at 30, 60, and 120 min with replacement of an equal volume of the appropriate buffer containing or lacking the compounds. Samples were stored at −20 °C until analysis. After 120 min, lucifer yellow was added to the donor chamber, with additional sampling as above at 10, 20, and 30 min. Lucifer yellow was analyzed by fluorescence (excitation 450 nm, emission 528 nm) in a Synergy 2 microplate reader. Monolayer tight junctions and integrity were confirmed by measurement of transepithelial electrical resistances >400 ohm·cm^2 and by lucifer yellow permeabilities of $< 1 \times 10^{-6}$ cm/s. Buffer samples (200 μL) were mixed with acetonitrile (100 μL) and acetic acid (2 μL), vortexed and centrifuged at 4 °C for 5 min at 12 000 rcf. Supernatants (100 μL) were injected onto an Alltech Alltima HP C18 4.6 × 100 mm 3 μm column and eluted with 38% acetonitrile, 62% aqueous (1% acetic acid in water) at 1.0 mL/min. To improve sensitivity over UV detection, fluorescence (Waters 2475) at the excitation/emission wavelengths of 443/533 and 274/305 (nm) for **1** and **14**, respectively, was also detected. Permeability was determined according to Fick's Law. Efflux transport activity was defined as a permeability directional ratio (efflux ratio) ≥ 2.

Acknowledgment. We thank Dr. George M. Martin at the University of Washington, Seattle, for kindly providing the MC65 cells. We acknowledge Dr. Pallabi Mitra and Zhenxian Zhang for their help with Caco-2 permeability experiments. We also acknowledge Dr. Ting Yang (Harvard Institute of Medicine) for the ML60 ELISA assay. The work was supported in part by Alzheimer's & Related Diseases Research Award Fund, Commonwealth of Virginia (S.Z.), and new faculty start-up funds from Virginia Commonwealth University (S.Z.).

References

(1) Hardy, J.; Selkoe, D. J. The amyloid hypothesis of Alzheimer's disease: progress and problems on the road to therapeutics. *Science* **2002**, *297*, 353–356.
(2) Pratico, D. Oxidative stress hypothesis in Alzheimer's disease: a reappraisal. *Trends Pharmacol. Sci.* **2008**, *29*, 609–615.
(3) Selkoe, D. J. Soluble oligomers of the amyloid beta-protein impair synaptic plasticity and behavior. *Behav. Brain Res.* **2008**, *192*, 106–113.
(4) Lue, L. F.; Kuo, Y. M.; Roher, A. E.; Brachova, L.; Shen, Y.; Sue, L.; Beach, T.; Kurth, J. H.; Rydel, R. E.; Rogers, J. Soluble amyloid beta peptide concentration as a predictor of synaptic change in Alzheimer's disease. *Am. J. Pathol.* **1999**, *155*, 853–862.
(5) McLean, C. A.; Cherny, R. A.; Fraser, F. W.; Fuller, S. J.; Smith, M. J.; Beyreuther, K.; Bush, A. I.; Masters, C. L. Soluble pool of Abeta amyloid as a determinant of severity of neurodegeneration in Alzheimer's disease. *Ann. Neurol.* **1999**, *46*, 860–866.
(6) King, M. E.; Kan, H. M.; Baas, P. W.; Erisir, A.; Glabe, C. G.; Bloom, G. S. Tau-dependent microtubule disassembly initiated by prefibrillar beta-amyloid. *J. Cell Biol.* **2006**, *175*, 541–546.
(7) Zhang, Y.; McLaughlin, R.; Goodyer, C.; LeBlanc, A. Selective cytotoxicity of intracellular amyloid beta peptide 1−42 through p53 and Bax in cultured primary human neurons. *J. Cell Biol.* **2002**, *156*, 519–529.
(8) Lal, R.; Lin, H.; Quist, A. P. Amyloid beta ion channel: 3D structure and relevance to amyloid channel paradigm. *Biochim. Biophys. Acta* **2007**, *1768*, 1966–1975.
(9) Green, K. N.; LaFerla, F. M. Linking calcium to Abeta and Alzheimer's disease. *Neuron* **2008**, *59*, 190–194.
(10) Gasparini, L.; Dityatev, A. Beta-amyloid and glutamate receptors. *Exp. Neurol.* **2008**, *212*, 1–4.
(11) Chafekar, S. M.; Baas, F.; Scheper, W. Oligomer-specific Abeta toxicity in cell models is mediated by selective uptake. *Biochim. Biophys. Acta* **2008**, *1782*, 523–531.
(12) Petersen, R. B.; Nunomura, A.; Lee, H. G.; Casadesus, G.; Perry, G.; Smith, M. A.; Zhu, X. Signal transduction cascades associated with oxidative stress in Alzheimer's disease. *J. Alzheimer's Dis.* **2007**, *11*, 143–152.
(13) Reddy, P. H.; Beal, M. F. Amyloid β, mitochondrial dysfunction and synaptic damage: implications for cognitive decline in aging and Alzheimer's disease. *Trends Mol. Med.* **2008**, *14*, 45–53.
(14) Fukui, H.; Moraes, C. T. The mitochondrial impairment, oxidative stress and neurodegeneration connection: reality or just an attractive hypothesis? *Trends Neurosci.* **2008**, *31*, 251–256.
(15) Cordy, J. M.; Hooper, N. M.; Turner, A. J. The involvement of lipid rafts in Alzheimer's disease. *Mol. Membr. Biol.* **2006**, *23*, 111–122.
(16) Kim, S. I.; Yi, J. S.; Ko, Y. G. Amyloid beta oligomerization is induced by brain lipid rafts. *J. Cell. Biochem.* **2006**, *99*, 878–889.
(17) Choo-Smith, L. P.; Garzon-Rodriguez, W.; Glabe, C. G.; Surewicz, W. K. Acceleration of amyloid fibril formation by specific binding of Abeta-(1−40) peptide to ganglioside-containing membrane vesicles. *J. Biol. Chem.* **1997**, *272*, 22987–22990.
(18) Atwood, C. S.; Moir, R. D.; Huang, X.; Scarpa, R. C.; Bacarra, N. M.; Romano, D. M.; Hartshorn, M. A.; Tanzi, R. E.; Bush, A. I. Dramatic aggregation of Alzheimer abeta by Cu(II) is induced by conditions representing physiological acidosis. *J. Biol. Chem.* **1998**, *273*, 12817–12826.
(19) Wakabayashi, M.; Okada, T.; Kozutsumi, Y.; Matsuzaki, K. GM1 ganglioside-mediated accumulation of amyloid β-protein on cell membrane. *Biochem. Biophys. Res. Commun.* **2005**, *328*, 1019–1023.
(20) Wang, S. S.; Rymer, D. L.; Good, T. A. Reduction in cholesterol and sialic acid content protects cells from the toxic effects of beta-amyloid peptides. *J. Biol. Chem.* **2001**, *276*, 42027–42034.

(21) Ariga, T.; McDonald, M. P.; Yu, R. K. Role of ganglioside metabolism in the pathogenesis of Alzheimer's disease--a review. *J. Lipid Res*. **2008**, *49*, 1157–1175.
(22) Oda, A.; Tamaoka, A.; Araki, W. Oxidative stress up-regulates presenilin 1 in lipid rafts in neuronal cells. *J. Neurosci. Res*. **2010**, *88*, 1137–1145.
(23) Panza, F.; Solfrizzi, V.; Frisardi, V; Imbimbo, B. P.; Capurso, C.; D'Introno, A.; Colacicco, A. M.; Seripa, D.; Vendemiale, G.; Capurso, A.; Pilotto, A. Beyond the neurotransmitter-focused approach in treating Alzheimer's disease: drugs targeting beta-amyloid and tau protein. *Aging Clin. Exp. Res*. **2009**, *21*, 386–406.
(24) Sabbagh, M. N. Drug development for Alzheimer's disease: where are we now and where are we headed? *Am. J. Geriatr. Pharmacother*. **2009**, *7*, 167–185.
(25) Cavalli, A.; Bolognesi, M. L.; Minarini, A.; Rosini, M.; Tumiatti, V.; Recanatini, M.; Melchiorre, C. Multi-target-directed ligands to combat neurodegenerative diseases. *J. Med. Chem*. **2008**, *51*, 347–372.
(26) Amit, T.; Avramovich-Tirosh, Y.; Youdium, M. B.; Mandel, S. Targeting multiple Alzheimer's disease etiologies with multimodal neuroprotective and neurorestorative iron chelators. *FASEB J*. **2008**, *22*, 1296–1305.
(27) Kim, Y. S.; Lee, J. H.; Ryu, J.; Kim, D. J. Multivalent & multifunctional ligands to β-amyloid. *Curr. Pharm. Des*. **2009**, *15*, 637–658.
(28) Portoghese, P. S. From models to molecules: opioid receptor dimers, bivalent ligands, and selective opioid receptor probes. *J. Med. Chem*. **2001**, *44*, 2259–2269.
(29) Yang, F.; Lim, G. P.; Begum, A. N.; Ubeda, O. J.; Simmons, M. R.; Ambegaokar, S. S.; Chen, P. P.; Kayed, R.; Glabe, C. G.; Frautschy, S. A.; Cole, G. M. Curcumin inhibits formation of amyloid beta oligomers and fibrils, binds plaques, and reduces amyloid in vivo. *J. Biol. Chem*. **2005**, *280*, 5892–5901.
(30) Ray, B.; Lahiri, D. K. Neuroinflammation in Alzheimer's disease: different molecular targets and potential therapeutic agents including curcumin. *Curr. Opin. Pharmacol*. **2009**, *9*, 434–444.
(31) Frautschy, S. A.; Cole, G. M. Why pleiotropic interventions are needed for Alzheimer's disease. *Mol. Neurobiol*. **2010**, *41*, 392–409.
(32) Kim, J.; Lee, H. J.; Lee, K. W. Naturally occuring phytochemicals for the prevention of Alzheimer's disease. *J. Neurochem*. **2010**, *112*, 1415–1430.
(33) Rajendran, L.; Schneider, A.; Schlechtingen, G.; Weidlich, S.; Ries, J.; Braxmeier, T.; Schwille, P.; Schulz, J. B.; Schroeder, C.; Simons, M.; Jennings, G.; Knolker, H. J.; Simons, K. Efficient inhibition of the Alzheimer's disease beta-secretase by membrane targeting. *Science* **2008**, *320*, 520–523.
(34) Hussey, S. L.; He, E.; Peterson, B. R. Synthesis of chimeric 7alpha-substituted estradiol derivatives linked to cholesterol and cholesterylamine. *Org. Lett*. **2002**, *4*, 415–418.
(35) Kolb, H. C.; Sharpless, K. B. The growing impact of click chemistry on drug discovery. *Drug Discovery Today* **2003**, *8*, 1128–1137.
(36) Ouberai, M.; Dumy, P.; Chierici, S.; Garcia, J. Synthesis and biological evaluation of clicked curcumin and clicked KLVFFA conjugates as inhibitors of β-amyloid fibril formation. *Bioconjugate Chem*. **2009**, *20*, 2123–2132.
(37) Pabon, H. J. J. Synthesis of curcumin and related compounds. *Rec. Trav. Chim*. **1964**, *83*, 379–386.
(38) Sopher, B. L.; Fukuchi, K.; Smith, A. C.; Leppig, K. A.; Furlong, C. E.; Martin, G. M. Cytotoxicity mediated by conditional expression of a carboxyl-terminal derivative of the beta-amyloid precursor protein. *Brain Res. Mol. Brain Res*. **1994**, *26*, 207–217.
(39) Maezawa, I.; Hong, H. S.; Wu, H. C.; Battina, S. K.; Rana, S.; Iwamoto, T.; Radke, G. A.; Petterson, E.; Martin, G. M.; Hua, D. H.; Jin, L. W. A novel tricyclic pyrone compound ameliorates cell death associated with intracellular amyloid-β oligomeric complexes. *J. Neurochem*. **2006**, *98*, 57–67.
(40) Sopher, B. L.; Fukuchi, K. I.; Kavanagh, T. J.; Furlong, C. E.; Martin, G. M. Neurodegenerative mechanisms in Alzheimer's disease. *Mol. Chem. Neuropathol*. **1996**, *29*, 153–167.
(41) Xia, W.; Zhang, J.; Kholodenko, D.; Citron, M.; Podlisny, M. B.; Teplow, D. B.; Haass, C.; Seubert, P.; Koo, E. H.; Selkoe, D. J. Enhanced production and oligomerization of the 42-residue amyloid beta-protein by Chinese hamster ovary cells stably expressing mutant presenilins. *J. Biol. Chem*. **1997**, *272*, 7977–7982.
(42) Walsh, D. M.; Tseng, B. P.; Rydel, R. E.; Podlisny, M. B.; Selkoe, D. J. The oligomerization of amyloid beta-protein begins intracellularly in cells derived from human brain. *Biochemistry* **2000**, *39*, 10831–10839.
(43) Kayed, R.; Head, E.; Thompson, J. L.; McIntire, T. M.; Milton, S. C.; Cotman, C. W.; Glade, C. G. Common structure of soluble amyloid oligomers implies common mechanism of pathogenesis. *Science* **2003**, *18*, 486–489.
(44) Lantto, T. A.; Colucci, M.; Zavadova, V.; Hiltunen, R.; Raasmaja, A. Cytotoxicity of curcumin, resveratrol and plant extracts from basil, juniper, laurel and parsley in SH-SY5Y and CV1-P cells. *Food Chem*. **2009**, *117*, 405–411.
(45) Oyama, Y.; Hayashi, A.; Ueha, T.; Maekawa, K. Characterization of 2′,7′-dichlorofluorescin fluorescence in dissociated mammalian brain neurons: estimation on intracellular content of hydrogen peroxide. *Brain Res*. **1994**, *635*, 113–117.
(46) Forrest, V. J.; Kang, Y. H.; McClain, D. E.; Robinson, D. H.; Ramakrishnan, N. Oxidative stress-induced apoptosis prevented by Trolox. *Free Radical Biol. Med*. **1994**, *16*, 675–684.
(47) Woltjer, R. L.; Nghiem, W.; Maezawa, I.; Milatovic, D.; Vaisar, T.; Montine, K. S.; Montine, T. J. Role of glutathione in intracellular amyloid-β precursor protein/carboxy-terminal fragment aggregation and associated cytotoxicity. *J. Neurochem*. **2005**, *93*, 1047–1056.
(48) Adachi, Y.; Suzuki, H; Sugiyama, Y. Comparative studies on in vitro methods for evaluating in vivo function of MDR1 P-glycoprotein. *Pharm. Res*. **2001**, *18*, 1660–1668.
(49) Mensch, J.; Melis, A.; Mackie, C.; Verreck, G.; Brewster, M. E.; Augustijns, P. Evaluation of various PAMPA models to identify the most discriminating method for the prediction of BBB permeability. *Eur. J. Pharm. Biopharm*. **2010**, *74*, 495–502.
(50) Garberg, P.; Ball, M.; Borg, N.; Cecchelli, R.; Fenart, L.; Hurst, R. D.; Lindmark, T.; Mabondzo, A.; Nilsson, J. E.; Raub, T. J.; Stanimirovic, D.; Terasaki, T.; Oberg, J. O.; Osterberg, T. In vitro models for the blood-brain barrier. *Toxicol. In Vitro* **2005**, *19*, 299–334.
(51) Poller, B.; Gutmann, H.; Krahenbuhl, S.; Weksler, B.; Romero, I.; Couraud, P. O.; Tuffin, G.; Drewe, J.; Huwyler, J. The human brain endothelial cell line hCMEC/D3 as a human blood-brain barrier model for drug transport studies. *J. Neurochem*. **2008**, *107*, 1358–1368.
(52) Lohmann, C.; Huwel, S.; Galla, H. J. Predicting blood-brain barrier permeability of drugs: evaluation of different in vitro assays. *J. Drug Target* **2002**, *10*, 263–276.
(53) Usta, M.; Wortelboer, H. M.; Vervoort, J.; Boersma, M. G.; Rietjens, I. M.; van Bladeren, P. J.; Cnubben, N. H. Human glutathione S-transferase-mediated glutathione conjugation of curcumin and efflux of these conjugates in Caco-2 cells. *Chem. Res. Toxicol*. **2007**, *20*, 1895–1902.
(54) Giacomini, K. M.; Huang, S. M.; Tweedie, D. J.; Benet, L. Z.; Brouwer, K. L.; Chu, X.; Dahlin, A.; Evers, R.; Fischer, V.; Hillgren, K. M.; Hoffmaster, K. A.; Ishikawa, T.; Keppler, D.; Kim, R. B.; Lee, C. A.; Niemi, M.; Polli, J. W.; Sugiyama, Y.; Swaan, P. W.; Ware, J. A.; Wright, S. H.; Wah Yee, S.; Zamek-Gliszczynski, M. J.; Zhang, L. Membrane transporters in drug development. *Nat. Rev. Drug Discovery* **2010**, *9*, 215–236.
(55) Wang, Y. J.; Thomas, P.; Zhong, J. H.; Bi, F. F.; Kosaraju, S.; Pollard, A.; Fenech, M.; Zhou, X. F. Consumption of grape seed extract prevents amyloid-beta deposition and attenuates inflammation in brain of an Alzheimer's disease mouse. *Neurotoxic. Res*. **2009**, *15*, 3–14.
(56) Garcia-Alloza, M.; Borrelli, L. A.; Rozkalne, A.; Hyman, B. T.; Bacskai, B. J. Curcumin labels amyloid pathology in vivo, disrupts existing plaques, and partially restores distorted neuritis in an Alzheimer's mouse model. *J. Neurochem*. **2007**, *102*, 1095–1104.
(57) Ryu, E. K.; Choe, Y. S.; Lee, K. H.; Choi, Y.; Kim, B. T. Curcumin and dehydrozingerone derivatives: synthesis, radiolabeling, and evaluation for beta-amyloid plaque imaging. *J. Med. Chem*. **2006**, *49*, 6111–6119.